Investigation of the Selective Laser Melting process with tungsten metal powder

A.T. Sidambe*, P. Fox*

* 1. Centre for Materials and Structures, School of Engineering, University of Liverpool, Brownlow Hill, Liverpool, L69 3GH UK

Abstract

Selective Laser Melting (SLM) is a leading Additive Manufacturing (AM) technology used for high value low volume manufacturing. It is currently used commercially for processing of steels, titanium, nickel- and aluminum-alloys in medical and aerospace industries. It is not used currently for refractory metals, mainly because of the intrinsic problems of processing higher melting point materials but also due to the process being driven slowly by the industries involved. Successful SLM processing requires development of material specific processing parameters that differ between materials and so the system must be developed to match each material used. In this study, processing of tungsten is considered for the production of solid and porous parts. The study also considers the role of the pure tungsten powder interaction with processing conditions within SLM. The process quality is quantified in terms of porosity, integrity and microstructure. The reasons why the parameters used have the effects observed is discussed and the effects on future development of this technology in this field is discussed.

Keywords

Selective Laser Melting, Tungsten, Refractory metals, Additive Manufacturing, High-temperature, 3D printing.

Introduction

During the last two decades powder based additive manufacturing (AM) processes such as selective laser melting (SLM) have emerged as alternative techniques to conventional methods (eg machining and casting) because of their ability to reduce the cost of production, particularly for complex shapes, as they enable the production of one off near net shape components [1, 2] [3] [4]. SLM, often also referred to as direct metal laser sintering (DMLS) or selective laser sintering (SLS) is often preferred because it can produce functional custom specific, complex, solid or lattice components quickly and without tooling [1]. In the SLM system, a high-powered laser with a power of 200 to 400W is used to fuse metal powder into a solid component based on a 3D CAD file. Components are built one layer at a time using the additive method with the layer thickness typically in the range of 30 µm [5-8]. Figure 1 shows a schematic diagram for the SLM process.

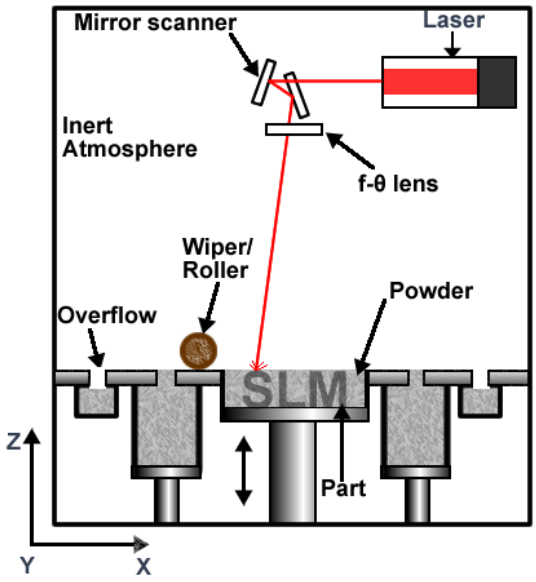

Figure 1: Schematic overview of the selective laser melting (SLM) process

Refractory Metals

The application of SLM to the processing of refractory metals has so far been limited. Refractory metals are high strength, high temperature metals which have excellent corrosion resistance. Their applications today include medical implants, rocket nozzles and support hardware [9, 10]. The limitations of the applications has historically been attributed to manufacturing complexity, material cost and material density. Additive manufacturing techniques such as SLM can be used to overcome these problems, leading to an increase in the application of refractory metals, with these materials used in a novel ways. For example, SLM can be used for the production of cellular structures that can deliver the strength and temperature properties that refractory metals provide, whilst reducing the overall mass of the component – one of the key application barriers. Refractory metals are already widely processed using powder metallurgy processes such as Hot Isostatic Pressing (HIP) meaning that powder supply is already available. Therefore processing of refractory metals via SLM although technically challenging, would lead to an advantage in these high value manufacturing sectors.

Tungsten

Tungsten has a very high melting point (3422 °C), high boiling point (5700 ± 200 °C), low vapor pressure and low thermal expansivity. It is for this reason that tungsten is used in ultra-high temperature applications in many technology fields such as military, electro vacuum, crucible and heating elements [11]. Tungsten also has a high density (19.2 g/cm^3) and this gives it superior radiation attenuation characteristics, which makes tungsten ideal for use as shielding and in pinhole collimators [12]. However the hardness and strength of tungsten hinders the processing of complicated shaped parts with small dimensions. In these cases, traditional metal working techniques such as milling, casting or pressing cannot be used [11].

The challenges of using conventional fabrication with tungsten has led to a number of studies that investigated the use of additive manufacturing. In one of the early studies, Zhong et al. [13] reported that pure tungsten could not be used to fabricate a collimator, using a blown powder process called Laser Engineered Net Shaping (LENS™), due to the metals high melting point [13], however, they reported that the use of a tungsten nickel alloy powder was successful. In a later study, Ebert et al. (2012) investigated the laser micro sintering of tungsten and demonstrated that the density of the tungsten parts increased with increased applied laser energy [14], showing that with sufficient power processing should be possible. A year later, Deprez et al. (2013) produced a complex collimator with a large number of oblique pinholes from pure tungsten powder using selective laser melting [12]. More recently, the intrinsic tungsten properties and the laser processing parameters have been found to be important in determining the properties of the SLM produced parts. A study by Zhou et al. (2015) identified oxidation as a phenomenon that would hinder successful SLM processing and which must be avoided [9].

In this study, we identify more of the barriers that limit the effectiveness of SLM processing of pure tungsten and then evaluate the performance. A further study was also conducted to evaluate the development of cellular refractory metal structures for industrial applications including an analysis of some tungsten applications.

Experimental

Selective Laser Melting of Tungsten

A Renishaw AM125 system manufactured by Renishaw (Stone, UK) which employs a high powered ytterbium fibre laser with a wavelength of 1070 nm, a maximum laser power of 200 W in continuous wave mode, a maximum laser scanning speed of 2000 mm/s and a laser beam diameter of 43 µm at the powder surface was used to melt plasma-densified tungsten powder (W45) supplied by Tekna Advanced Materials (Macon, France) under an argon atmosphere. The laser beam has a Gaussian intensity profile and has sufficient intensity to melt refractory metals such as tungsten when the focus offset is set on the central part of the geometry [15]. A commercially pure titanium substrate was used for the SLM experiments. Figure 2 shows the profiling optimisation that was carried out to achieve the optimal focus offset using an Ophir Photonics Spiricon SP620 beam profiler (Jerusalem,Israel).

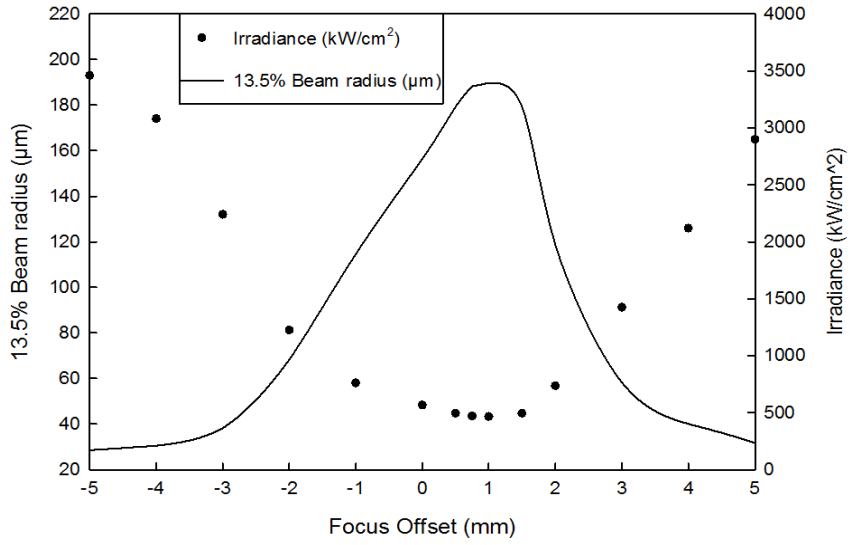

Figure 2: Laser beam profiling on the SLM 125 machine

Figure 3 (a) is a scanning electron micrograph (SEM) showing the highly spherical powder morphology of the tungsten powder. The analysis was carried out using a Jeol 6610 (Akishima, Japan) scanning electron microscope at 20kV. Figure 3 (b) shows the powder particle distribution of the sub 45µm powder. The flow properties of the powder were also established through the 'conical' shape of the powder which were confirmed through measurements of the angle of repose (25.6°) which were carried out by LPW Technology (Runcorn, UK).

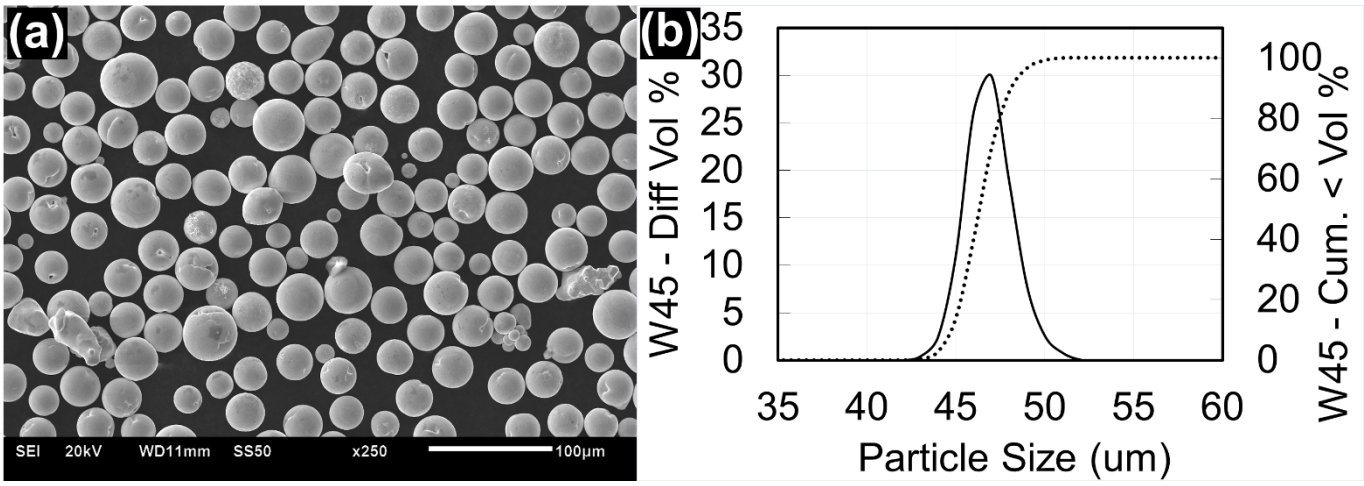

Figure 3: Powder morphology (a) and powder particle distribution (b) for Tungsten (W45).

Table 1 shows the chemical composition of the powders as documented in the supplier power certification. It can be seen from Table 1 that the initial levels of oxygen in the powder are low and show high purity.

The strategy for investigating the melting of the tungsten powder was based on initially carrying out single track melting. This was done by studying the effect of changing the scan speed on the formation of fusion lines and single tracks. This was followed by the study focused on the single layer melting with the view to study the effect of the scan strategy on the overlap (hatch spacing).

W45 - Chemical Composition (wt%)						
W	Al	Ta	Ti	O	Mo	Residual
>99.9	0.001	0.003	0.001	0.009	0.003	<0.001

Table 1: Chemical composition of the tungsten (W45) powder used in the SLM studies.

SLM Processing Parameter	Point Distance (µm)	Exposure Time (µs)	Apparent Speed (mm/s)	3D volume energy density (J/mm^3)	Hatch Space (mm)
A	20	200	100	578	0.115
B	20	200	100	434	0.155
C	29	200	145	399	0.115
D	29	200	145	299	0.155

Table 2: Summary of the processing parameters used to manufacture four different tungsten SLM components

Finally, tungsten block components (L=10mm, W=10mm and H=5mm) were manufactured using SLM. Table 2 is a summary of the four sets of processing parameters used to manufacture the different tungsten SLM components with a layer thickness of 30µm. The 3D laser energy density was derived from 3D specific energy input and it is obtained by combining laser power, laser scan speed, powder layer thickness, and hatch spacing [16-19]. This 3D formulation can be seen as Equation 1 below:

$$\mathcal{E}_{Density} = \frac{P_{Laser}}{v_{scan} . S_{hatch} . t_{layer}} \quad \text{Eqn 1}$$

$\mathcal{E}_{\text{Density}}$ is the 3 dimensional input laser energy density, P_{Laser} is the laser power, v_{scan} is the laser scan speed, s_{hatch} is the hatch spacing and t_{layer} is the layer thickness. The Renishaw AM125 machine uses a point exposure scan strategy which implies that the laser does not remain continuously on when incident on powder material. Therefore the scan speed was derived from the point distance and the exposure time used in the parameters.

After the tungsen blocks were fabricated, they were subjected to analysis alongside tungsten powder material on a Rigaku MiniFlex X-Ray diffraction (XRD) instrument (Tokyo, Japan). The tungsten block SLM specimens were also sectioned, ground, polished to 1µm in Al_20_3 powders and analysed for porosity levels using the light optical microscopy (LOM) and ImageJ image processing software. A selection of the polished specimens were then subjected to electrolytic etching and that was carried out using a 5% sodium hydroxide solution in a cooled electrolytic cell, at a typical temperature of -20°C at 40V. The etched samples were also analysed using LOM and SEM to study preferred growth direction of grains during the SLM process.

Results

Single track melting

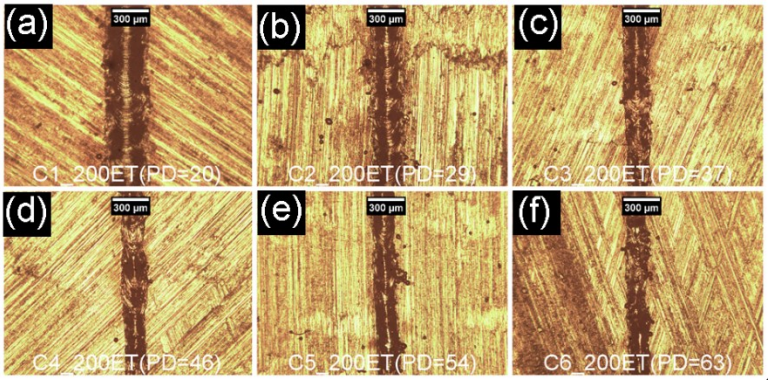

Figure 4: Single track melting results of tungsten powder using different scan parameters.

Figure 4 shows optical micrographs of single track melting results of tungsten powder using different scan parameters. Figure 4 shows that when the energy density is insufficient, the surface tension causes breaks which leads to thin melt tracks (Figure 4 f). With the increase of energy input, continuous melt tracks of regular width are formed (Figure 4 c). With further increase in energy density there is an increase in the melt volume and a decrease of the melt viscosity and melt hydrodynamics (driven by Marangoni effect) becomes more important [19]. Also the decrease in the scanning speed causes the heat affected zone to become larger causing more powder to melt (Figure 4 a).

Figure 5 shows the quantification of the melted line width for the tungsten as a function of the scanning speed. Figure 6 shows line width as a function of 1D line energy density (laser power/unit speed). It can be seen from Figure 5 and Figure 6 that the geometrical dimensions of the melt tracks are dependent on scan speed and on the energy density. This is useful information which can be used to define the threshold for the energy density. From Figure 5 and Figure 6, it is evident that for the given laser power the temperature and the volume of the molten powder is higher at lower scanning speeds and higher energy densities. The result also confirms that the surface tension coefficient as well as melt viscosity decrease with temperature [19] in the SLM of tungsten.

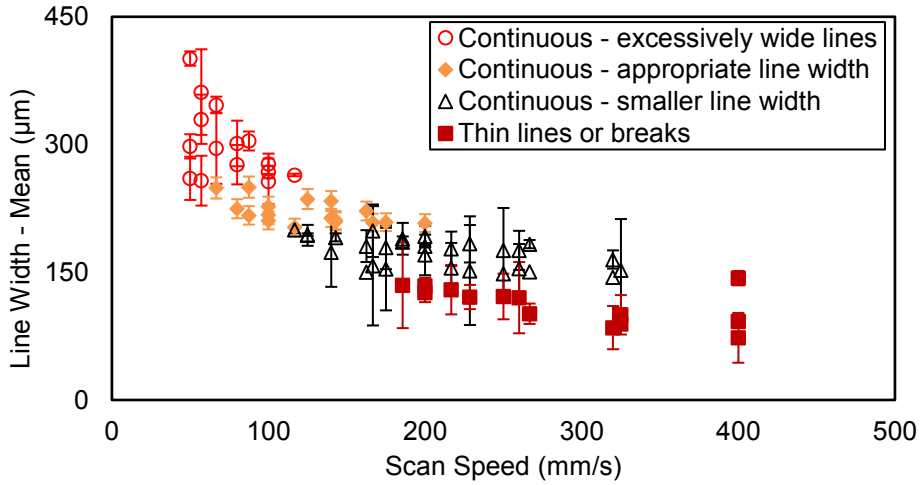

Figure 5: Line width vs scan speed for tungsten (W45) powder

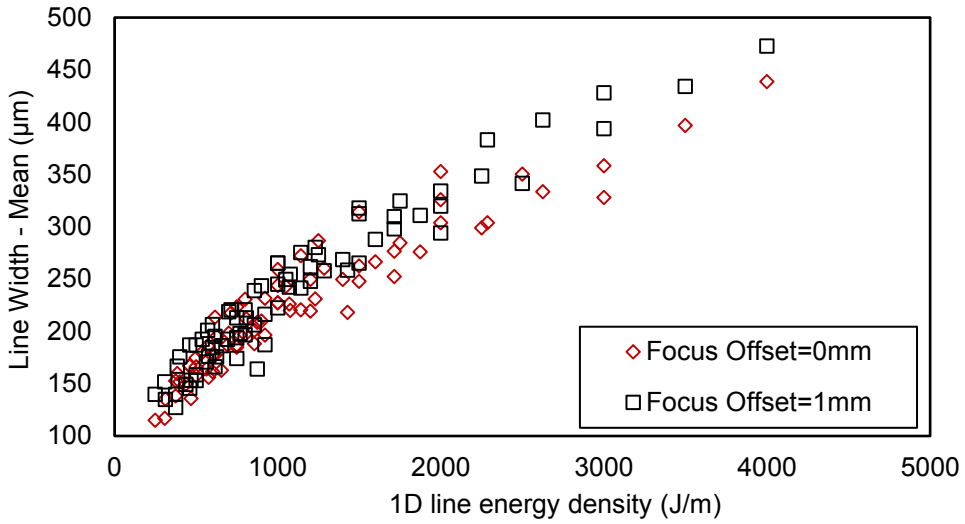

Figure 6: Line width vs 1D line energy density for tungsten (W45) powder

Single layer hatch patterns

In the 3 dimensional melting of powder, the laser power, scan speed or velocity, hatch distance, and layer thickness can be modified to increase or decrease the 3D laser energy density in order to control the powder fusion. These process parameters have been used in this study with powder material properties of tungsten having been taken into consideration and the threshold determined by the previously outlined studies. Figure 7 shows the single layer hatch patterns for tungsten using different processing parameters. Also shown in Figure 7 are the processing parameters based on Table 2. The result shows that at a given laser power, higher scan speed and larger hatch spacing reduce the size of the melt pool spreading in order to modify the overlap [20, 21]. The melt tracks in Figure 7 (b) and Figure 7 (d) indicate that there is in insufficient overlap of the scan tracks and this could result in fusion defects or porosity [21].

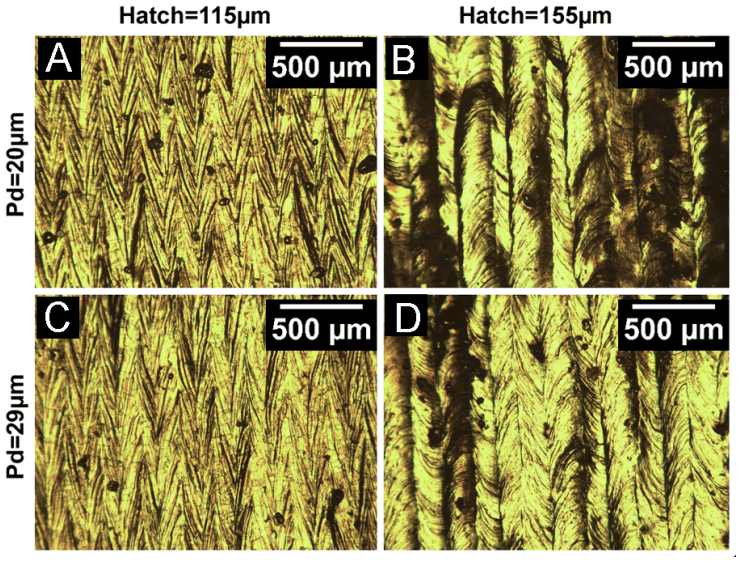

Figure 7: Single layer hatch patterns shown for tungsten (W45) using different processing parameters

SLM of Tungsten blocks

Figure 8 shows tungsten block components that were manufactured using the AM125 (L=50mm, W=10mm and H=5mm). The samples were successfully fabricated without any visible defects or delamination during the melting process and a relatively smooth surface was produced. Figure 9 shows the SEM images of the top surfaces (left) and side surfaces (right) of SLM tungsten fabricated using parameters in Table 2. However, at higher magnification cracks are visible within the manufactured components.

Figure 8: Tungsten components manufactured using SLM

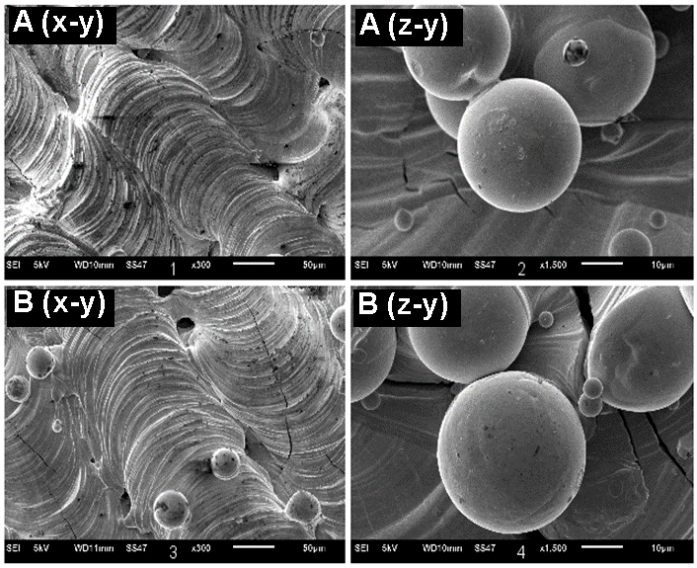

Figure 9: SEM's of the top surfaces (left) and side surfaces (right) of SLM tungsten (A and B) fabricated using parameters in Table 2.

X-Ray Diffraction Analysis

Figure 10 shows the results of the phase identification using an X-ray diffraction of the cross sectional x-y view of SLM samples (A and B) fabricated using parameters in Table 2. Compared to W powder, the diffraction peaks of the selective laser melted samples exhibit stronger intensity for the (100) and (211) planes. Thus, it can be deduced that growth from the melt pool formed under the laser beam favours solidification in a preferred orientation by a growth mechanism, leading to a columnargrain structure [22].

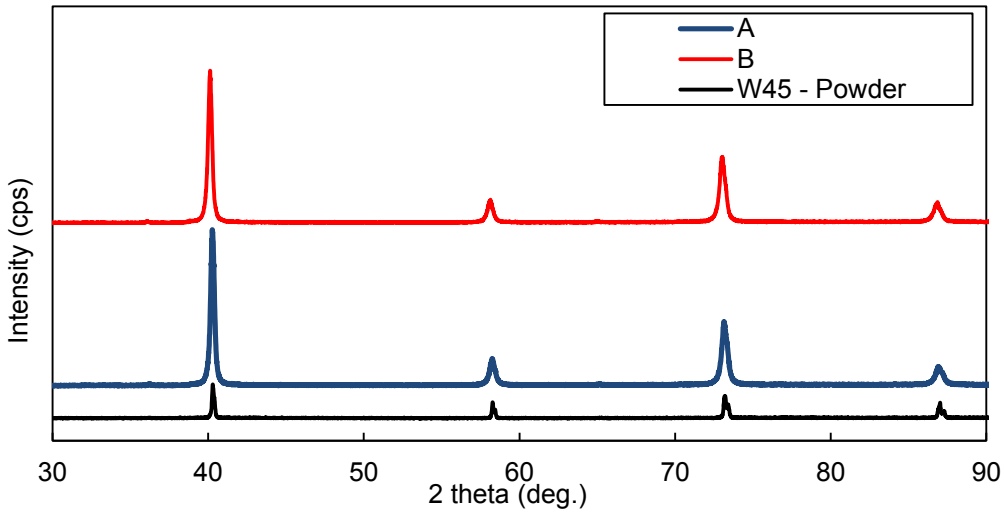

Figure 10: X-ray diffraction plot showing W powder as well as traces and peaks for SLM samples (A and B) fabricated using parameters in Table 2.

Density and Porosity

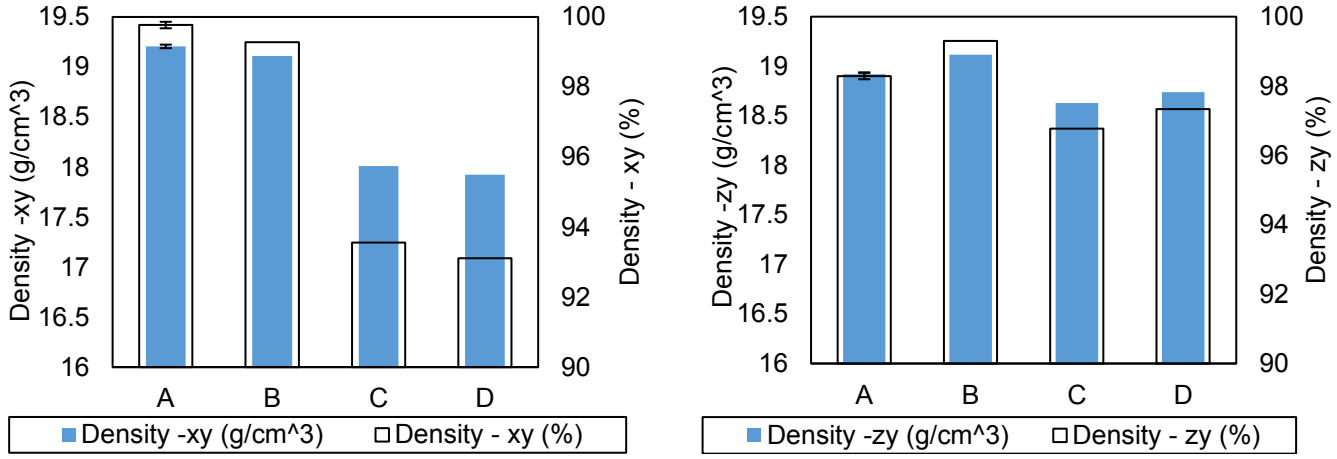

Figure 11: Optically determined density of the lateral view (x-y) and cross-section (z-y) view of four tungsten (W45) samples fabricated using different parameters in Table 2.

Figure 11 shows the results of the optically determined density of the cross-section view (x-y) and build direction view (z-y) of the four tungsten (W45) samples fabricated using different parameters. It can be seen from Figure 11 that specimens manufactured using the set of parameters A and B had the highest density. The energy density was higher in these samples (A and B) as can be seen from Table 2, particularly dominated by the short point distance of 20µm. The optical micrographs showing the porosity levels of the tungsten specimens fabricated by SLM can be seen in Figure 12. The micrographs confirm the density levels and the levels of integrity obtained and also show the effect of the different processing parameters.

Optical micrographs showing cross sectional (xy) and build direction (zy) grain structures are shown in Figure 13. Higher magnification SEM images of the grain alignment and crack initiation zones are shown in Figure 14 for both cross sectional (xy) and build direction (zy) views.

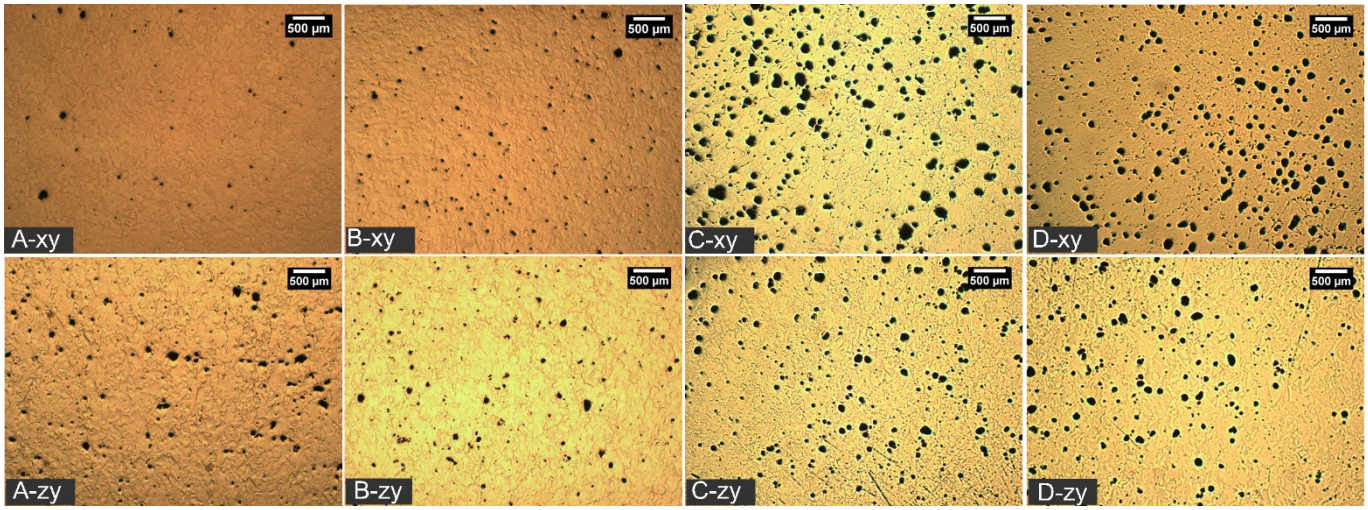

Figure 12: Optical micrographs showing the porosity levels of the tungsten specimens fabricated via SLM

Microstructure of SLM Tungsten

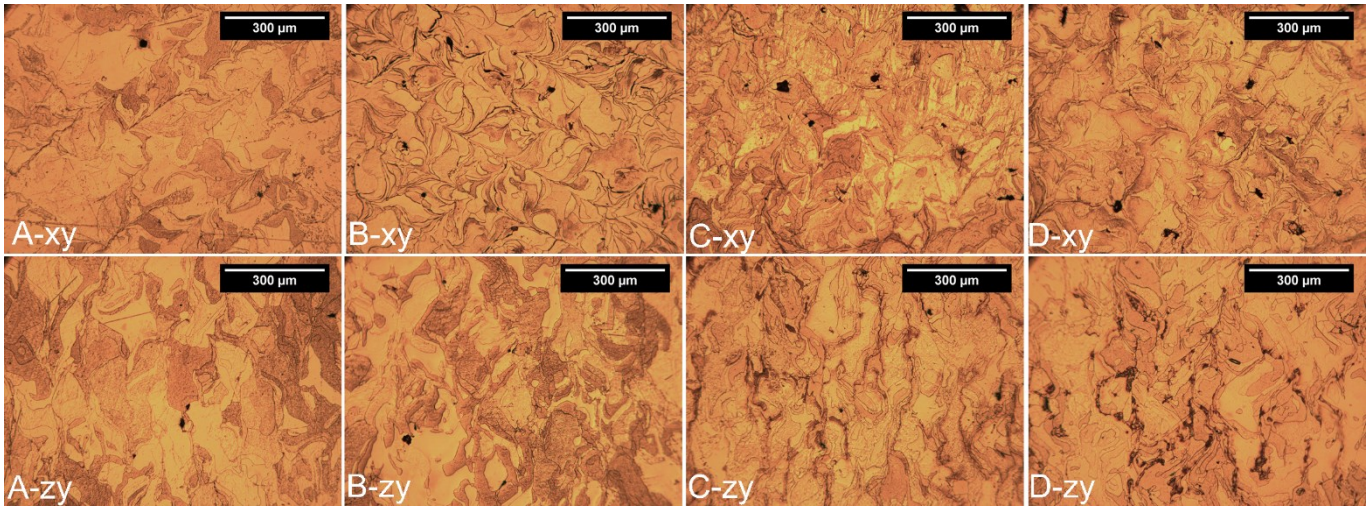

Figure 13: Optical micrographs showing cross sectional (1) and build direction (2) grain structures

Figure 13 and Figure 14 show that there is a preferential orientation of the grain structures, as predicted by the XRD data. When the LOM in Figure 13 is used to analyse cross sectional x-y direction, it can be seen that there is an organisation of grain texture in accordance with scan tracks. When the build direction (z-y) texture is analysed, it can be deduced that there is anisotropy as grains align along the build direction as expected because SLM is a layer by layer deposition, melting and freezing process. The SEM image in Figure 14 also shows the preferential grain growth and anisotropy between the cross-section and build direction. Also discernible from Figure 14 is that the grain separation is more pronounced in samples C and D which were manufactured using the point distance of 29µm.

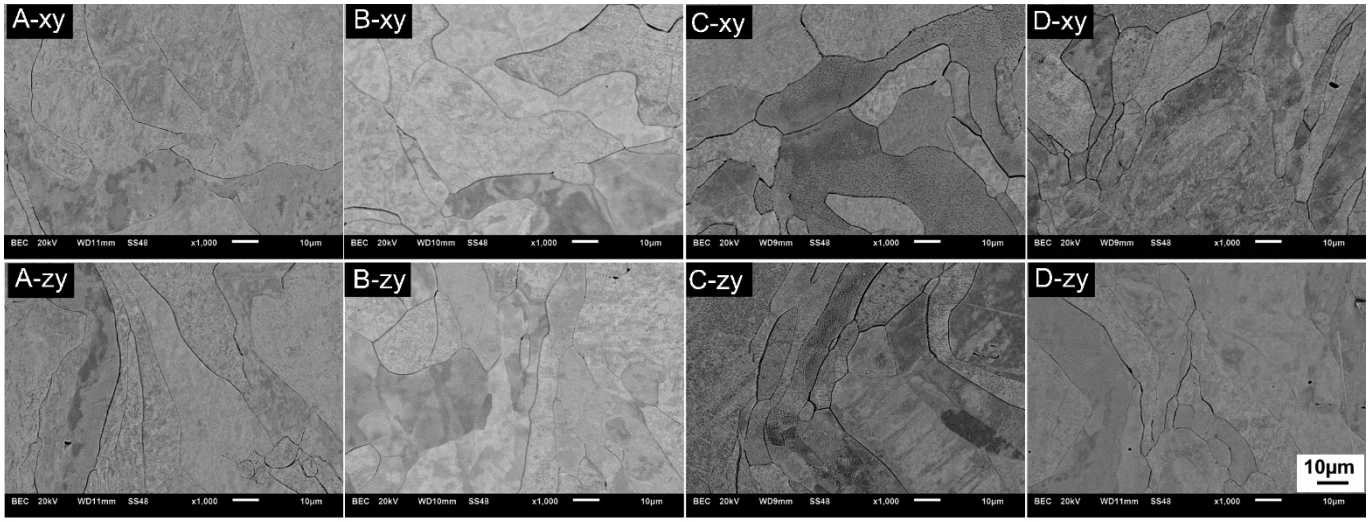

Figure 14: SEM's showing cross sectional (xy) and build direction (zy) grain structures.

Applications

Figure 15 shows a tungsten porous component manufactured using SLM. The manufacturing of the lattice structure demonstrates the suitability of SLM parameters for the lightweight components and future development of this technology in this field.

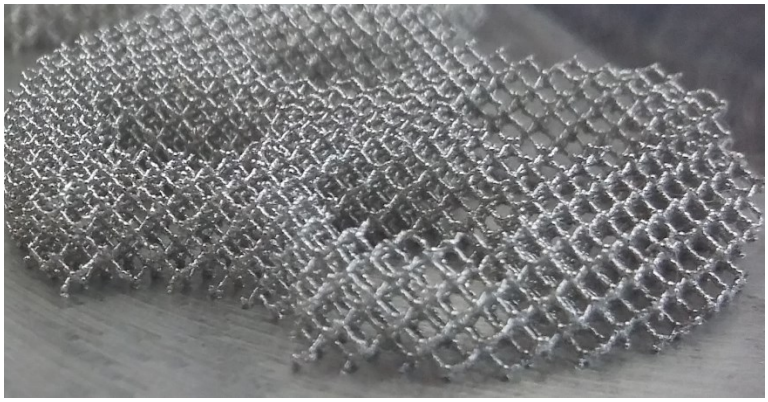

Figure 15: Tungsten porous component manufactured using SLM.

Discussion

Manufacture of pure tungsten samples by SLM is considered difficult due to the high melting point, high thermal conductivity, high viscosity and oxidation sensitivity. In this study we have optimised the parameters so that they overcome the high cohesive energy and high surface tension and reduce the balling phenomenon. The parameters used have taken into consideration the fact that tungsten has a high thermal conductivity and therefore is expected to cool very rapidly. The processing has also been carried out in an argon atmosphere to prevent oxidation which has been reported to lead to the formation of an oxide film on the surface of previously built solid tracks and at the bottom of the melt pools [9].

In this study it has been shown that the parameters for melting tungsten depend on the energy density and scan speed, and that point distance has a significant role overall. This study helped analyse the mode of melting for the tungsten powder. The processing started with the single melt pool strategy

where it was demonstrated that there is a dependence of single tracks dimensions on the energy density and this was decisive in the selection of the range of the energy density to use.

Conclusion

In this study, the processing of tungsten has been considered for the production of solid and porous parts. The role of the pure tungsten powder interaction with processing conditions within SLM has been demonstrated using a set of four different parameters which are equivalent to different energy densities. The process quality was quantified in terms of porosity and density where densities of up to 98% were achieved. The analysis of the microstructure has shown the anisotropy present in solids produced during the SLM processing of tungsten. The manufacture of a porous sample has demonstrated the applications and future developments of this technology in this field.

References

[1] A.T. Sidambe, *Materials* 7[12] 8168-8188 (2014).
[2] M.T. Andani, N. Shayesteh Moghaddam, C. Haberland, D. Dean, M.J. Miller, M. Elahinia, *Acta Biomaterialia* 10[10] 4058-4070 (2014).
[3] P. Fox, S. Pogson, C.J. Sutcliffe, E. Jones, *Surface & Coatings Technology* 202 5001–5007 (2008).
[4] A.T. Sidambe, I. Todd, P.V. Hatton, *Powder Metallurgy* 59[1] 57-65 (2016).
[5] O. Ivanova, C. Williams, T. Campbell, *Rapid Prototyping Journal* 19[5] 353-364 (2013).
[6] R. van Noort, *Dent. Mater.* 28[1] 3-12 (2012).
[7] N.J. Harrison, I. Todd, K. Mumtaz, *Acta Mater.* 94 59-68 (2015).
[8] P. Vora, K. Mumtaz, I. Todd, N. Hopkinson, *Additive Manufacturing* 7 12-19 (2015).
[9] X. Zhou, X.H. Liu, D.D. Zhang, Z.J. Shen, W. Liu, *J Mater Process Tech* 222 33-42 (2015).
[10] R. Wauthle, J. van der Stok, S. Amin Yavari, J. Van Humbeeck, J.P. Kruth, A.A. Zadpoor, H. Weinans, M. Mulier, J. Schrooten, *Acta Biomater* 14 217-25 (2015).
[11] R. Li, M. Qin, C. Liu, H. Huang, H. Lu, P. Chen, X. Qu, *International Journal of Refractory Metals and Hard Materials* 62, Part A 42-46 (2017).
[12] K. Deprez, S. Vandenberghe, K. Van Audenhaege, J. Van Vaerenbergh, R. Van Holen, *Med. Phys.* 40[1] 012501 (2013).
[13] M. Zhong, W. Liu, G. Ning, L. Yang, Y. Chen, *J Mater Process Tech* 147[2] 167-173 (2004).
[14] R. Ebert, F. Ullmann, D. Hildebrandt, J. Schille, L. Hartwig, S. Kloetzer, A. Streek, H. Exner, *J Laser Micro Nanoen* 7[1] 38-43 (2012).
[15] D. Faidel, D. Jonas, G. Natour, W. Behr, *Additive Manufacturing* 8 88-94 (2015).
[16] B. Brown, Characterization of 304L stainless steel by means of minimum input energy on the selective laser melting platform, Missouri University Of Science And Technology, 2014, p. 85.
[17] D. Gu, Y. Shen, *Materials & Design* 30[8] 2903-2910 (2009).
[18] Y.Q. Yang, J.B. Lu, Z.Y. Luo, D. Wang, *Rapid Prototyping Journal* 18[6] 482-489 (2012).
[19] I. Yadroitsev, P. Bertrand, I. Smurov, *Appl Surf Sci* 253[19] 8064-8069 (2007).
[20] L.E. Criales, Y.M. Arısoy, B. Lane, S. Moylan, A. Donmez, T. Özel, *Additive Manufacturing* 13 14-36 (2017).
[21] J.J.S. Dilip, G.D.J. Ram, T.L. Starr, B. Stucker, *Additive Manufacturing* 13 49-60 (2017).
[22] D. Zhang, Q. Cai, J. Liu, *Materials and Manufacturing Processes* 27[12] 1267-1270 (2012).